Separation of a Helium-Methane Mixture in Permeators with Two Types of Polymer Membranes

The separation of a He—CH_4 mixture containing 9.95 mol% He in permeator modules that incorporate two different types of polymer membranes was studied theoretically and experimentally. The membranes were symmetric dense capillaries of silicone rubber and asymmetric hollow fibers of cellulose triacetate. These membranes exhibit reverse selectivities for He and CH_4, silicone rubber being more permeable to CH_4, and cellulose triacetate more permeable to He. The simultaneous use of these two types of membranes in a permeator enhances the enrichment and recovery of He compared to the levels obtained with a single-membrane permeator utilizing either membrane alone. The experimental results were found to confirm the theoretical predictions, the agreement being better at the lower stage cuts.

J. E. Perrin, S. A. Stern
Department of Chemical Engineering
and Materials Science
Syracuse University
Syracuse, NY 13244

Introduction

Recent advances in membrane technology have given strong impetus to the study of new process design concepts for the separation of gas mixtures by selective permeation through polymer membranes. One such concept is the simultaneous use of two or more different types of membranes for a given separation process (Ohno et al., 1973–1978; Kimura et al., 1973). The membranes are chosen so as to exhibit specific selectivities for different components of a gas mixture to be separated. Thus, in order to separate a binary gas mixture, two different membranes are selected such that one membrane is more permeable to one component of the mixture, while the other membrane is more permeable to the second component. The membranes can be in the form of flat sheets, capillaries, or hollow fibers, and are usually mounted in devices or modules known as permeators. Analytical studies of gas separation in two-membrane permeators, i.e., those that enclose two different types of membranes, have been reported by several investigators for various operating conditions (Ohno, et al., 1977; Sirkar, 1980; Sengupta and Sirkar, 1984). More recently, mathematical models that consider three different flow patterns of the permeated (low-pressure) and unpermeated (high-pressure) gas streams in a two-membrane permeator have been developed by Perrin and Stern (1985). These flow patterns are: "perfect mixing," cocurrent flow, and countercurrent flow. The results of a parametric study based on the above models indicate that the separation and recovery of feed components achievable in a two-membrane permeator can be substantially larger than in a conventional single-membrane device.

The objective of the present study was to test the validity of models similar to those proposed by Perrin and Stern. Accordingly, this paper presents the results of an experimental investigation on the separation of a He-CH_4 mixture by means of two-membrane permeators enclosing both symmetric dense capillaries of silicone rubber and asymmetric hollow fibers of cellulose triacetate. Silicone rubber is more permeable to CH_4 than to He, while the opposite is true for cellulose triacetate. The He—CH_4 mixture contained 9.95 mol % He, and measurements were made at 30°C over a range of pressures and stage cuts. The permeators were operated under perfect mixing, cocurrent flow, and countercurrent flow conditions. The experimental results were compared with model predictions. The original models of Perrin and Stern (1985), which were derived for symmetric membranes, had to be modified to take into account the use of both symmetric and asymmetric membranes.

General Considerations

A simplified diagram of a two-membrane permeator module is shown in Figure 1. Consider the separation of a binary gas mixture of components A and B in this device. The permeator is

Correspondence concerning this paper should be addressed to S. A. Stern.
J. E. Perrin is currently with Innovative Membrane Systems, Inc., Norwood, MA 02062.

represented in Figure 1 as a black box separated into three compartments by two planar nonporous membranes, I and II. It is assumed that membrane I is more permeable to component A than to B, and that membrane II is more permeable to component B than to A. The gas mixture to be separated, the feed, is introduced into the middle compartment at a desired molar flow rate $L_{i(\ell)}$ and at a constant total pressure $p_{(\ell)}$. The mole fractions of components A and B in the feed are designated x_i^A and $x_i^B (=1 - x_i^A)$, respectively. A fraction of the feed is allowed to permeate simultaneously through each membrane into the upper and lower compartments of the permeator, which are maintained at the constant total pressures $p_{I(\ell)}$ $(<p_{(\ell)})$ and $p_{II(\ell)}$ $(<p_{(\ell)})$ respectively. The feed is thus partitioned into three product streams:

1. A permeated stream of molar flow rate $L_{Io(\ell)}$ and pressure $p_{I(\ell)}$, produced by membrane I and enriched in component A.
2. A permeated stream of molar flow rate $L_{IIo(\ell)}$ and pressure $p_{II(\ell)}$, produced by membrane II and depleted in component A, i.e., enriched in component B.
3. An unpermeated stream of molar flow rate $L_{o(\ell)}$ and pressure $p_{(\ell)}$, which can be either enriched or depleted in component A.

The mole fractions of component A in these three product streams will be designated y_{Io}^A, y_{IIo}^A, and x_o^A, respectively. Subscripts ℓ and ℓ' refer to the high- and low-pressure sides of the membranes, while subscripts i and o designate the permeator inlet and outlet, respectively. In addition, subscripts I and II refer to membranes I and II. The fraction θ of the feed that is allowed to permeate through each membrane is given by the relations:

$$\theta_I = L_{Io(\ell')}/L_{i(\ell)}, \quad \text{for membrane I,} \tag{1}$$

$$\theta_{II} = L_{IIo(\ell')}/L_{i(\ell)}, \quad \text{for membrane II,} \tag{2}$$

The fraction θ is generally referred to as the "stage cut."

The extent of separation achievable in a two-membrane permeator and the required membrane areas depend on the following operating variables:

- The feed flow rate
- The feed composition
- The nature of the membranes
- The temperature
- The pressures of the permeated and unpermeated gas streams in the permeator
- The stage cuts θ_I and θ_{II}
- The flow patterns of the permeated and unpermeated gas streams in the permeator.

For single-membrane permeators, the most often studied flow patterns have been the so-called "perfect mixing" (Weller and Steiner, 1950a,b; Stern et al., 1965; Stern and Walawender, 1969; Blaisdell and Kammermeyer, 1973), cross-flow (Weller and Steiner, 1950a,b; Walawender and Stern, 1972; Blaisdell and Kammermeyer, 1973), and cocurrent and countercurrent flow (Oishi et al., 1961; Walawender and Stern, 1972; Blaisdell and Kammermeyer, 1973; Pan and Habgood, 1974, 1978a,b; Stern and Wang, 1978). Analytical studies of gas separation in a perfectly mixed two-membrane permeator have been reported by Ohno et al. (1977) and by Sirkar (1980) for limited operating conditions. Sengupta and Sirkar (1984) have reported the results of an analytical and experimental study on the separation of a H_2—CO_2—N_2 mixture in a two-membrane permeator operating under cross-flow, cocurrent and countercurrent flow, and perfect mixing conditions. More recently, Perrin and Stern (1985) analyzed the separation of binary mixtures in such a permeator under the last three of the above-mentioned conditions.

Experimental Apparatus and Procedure

Permeability measurements with single-membrane permeators

The permeability to He and CH_4 of the tubular membranes used was determined from the steady-state permeation rates of the pure gases as well as of two different He—CH_4 mixtures. Two types of single-membrane permeators were constructed for

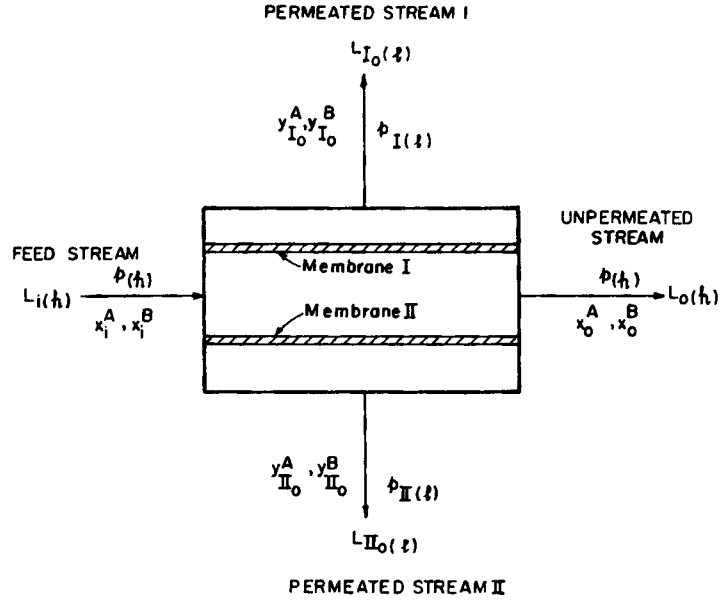

Figure 1. Diagram of two-membrane permeator.

this purpose, one containing only silicone rubber capillaries and the other only asymmetric hollow fibers of cellulose triacetate. The permeators were essentially high-pressure vessels in the form of shell-and-tube heat exchangers. The procedure for constructing these devices has been reported previously (McAfee, 1960; Stern et al., 1977).

The apparatus for measuring gas permeabilities consisted of a permeator module, the necessary valving, and the instrumentation required for the measurement and control of the operating variables, namely temperatures, pressures, flow rates, and gas compositions. Details of the entire apparatus have been reported elsewhere (Stern et al., 1977).

In order to perform permeability measurements with pure gases, He or CH_4 was admitted to a permeator at some desired overatmospheric pressure $p_{(\ell)}$ such that the capillaries or hollow fibers were pressurized externally (shell-side). The gas permeating through the walls of the capillaries or hollow fibers flowed axially inside these tubular membranes to the low-pressure outlet of the permeator. The pressure $p_{(\ell')}$ ($<p_{(\ell)}$) of the permeated gas stream, or permeate, was always close to atmospheric pressure at the permeator outlet. [The pressures $p_{(\ell)}$ and $p_{(\ell')}$ have been designated p_O and p_I respectively, in previous publications (Stern et al., 1977; Stern and Leone, 1980). The present nomenclature is more suitable for the subject matter under consideration.] Estimates of the pressure drop inside the capillaries and hollow fibers indicated that it was not significant under the experimental conditions. Six different permeator modules were constructed for the permeability measurements with pure gases: three of these permeators housed silicone rubber capillaries and the other three housed asymmetric hollow fibers of cellulose triacetate. The characteristics of the six permeators are listed in Table 1. The permeability of the capillaries and hollow fibers to He and CH_4 was characterized by a mean permeability coefficient $\bar{P}$, which is defined in a later section. $\bar{P}$ was determined as a function of the pressure difference Δp ($=p_{(\ell)} - p_{(\ell')}$ across the walls of the tubular membranes under isothermal conditions.

Permeability measurements were also made under steady-state conditions with two He—CH_4 mixtures containing 1.01 and 9.95 mol % He, respectively. During these measurements, the compositions of both the permeated (low-pressure) and unpermeated (high-pressure) product streams were continuously monitored at the permeator outlets. The tubular membranes, i.e., the capillaries and hollow fibers, were pressurized externally (shell-side) with the He—CH_4 mixtures studied. The flow pattern of the permeated and unpermeated streams inside the permeators was perfect mixing. This flow pattern was achieved by a suitable choice of permeator dimensions (Hill, 1977) and by employing low stage cuts ($\theta < 0.2$). The flow rates of the product streams were measured, depending on the magnitudes of the flow rates, with either a soap-bubble meter or by the water-displacement method. The flow rates of both streams were required in order to determine the stage cut during a measurement, i.e., the fraction of the feed permeating through the tubular membranes. The flow rate of the permeated stream also yielded the permeation rate of a He—CH_4 mixture through the walls of the tubular membranes.

The compositions of the permeated and unpermeated product streams were analyzed with a Varian 3700 gas chromatograph in conjunction with a recording integrator made by Hewlett-Packard Co. Details of the analysis have been reported by Perrin (1986).

The permeability measurements with He—CH_4 mixtures yielded permeability coefficients $\bar{P}$ for He and CH_4 in silicone rubber capillaries and asymmetric hollow fibers of cellulose triacetate as a function of Δp and composition under isothermal conditions.

Gas separation measurements with two-membrane permeators

The separation of a He—CH_4 mixture that contained 9.95 mol % He was studied by means of six two-membrane permeators. These permeators enclosed *both* symmetric dense capillaries of silicone rubber and asymmetric hollow fibers of cellulose triacetate, the two types of membranes being intermixed. The construction of a two-membrane permeator was similar to that of a single-membrane permeator, except that one of the tube sheets, or headers, in the former was provided with dual outlets for two permeated product streams instead of a single stream (Perrin, 1986); this is shown in Figure 2. The characteristics of the six two-membrane permeators used are listed in Table 2.

Experimental Materials

Pure gases

Pure He, CH_4, and N_2 were obtained from the Linde Division of Union Carbide Corp. He and CH_4 were employed for the separation studies, while N_2 was used as carrier gas for chromatographic analyses. The purity of these gases was stated by the

Table 1. Characteristics of Single-Membrane Permeators

Permeator Module	Tubular Membranes: Type	Number N	Effective Area, A cm^2
1	Silicone rubber,	20	40.8
2	symmetric (dense)	30	55.3
3	capillaries*	20	44.5
4	Cellulose triacetate,	36	58.2
5	asymmetric hollow	40	60.1
6	fibers**	40	62.3

*OD = 635 μm (25×10^{-3} in); ID = 305 μm (12×10^{-3} in)
**OD = 245 μm (9.65×10^{-3} in); ID = 69 μm (2.72×10^{-3} in)
The permeators differed in length.

Table 2. Characteristics of Two-Membrane Permeators

Permeator Module	Tubular Membranes: Number N_I^*	Effective Area, A_I cm^{2*}	Number N_{II}^{**}	Effective Area, A_{II} cm^{2**}	Ratio A_I/A_{II} ($=1/R$)
1	125	342.3	10	50.6	6.76
2	78	244.6	12	69.5	3.52
3	141	363.5	40	188.1	1.93
4	125	718.8	10	106.2	6.77
5	78	538.2	12	153.0	3.52
6	141	981.4	40	508.1	1.93

*I: Cellulose triacetate, asymmetric hollow fibers
**II: Silicone rubber, symmetric (dense) capillaries
The permeators differed in length.

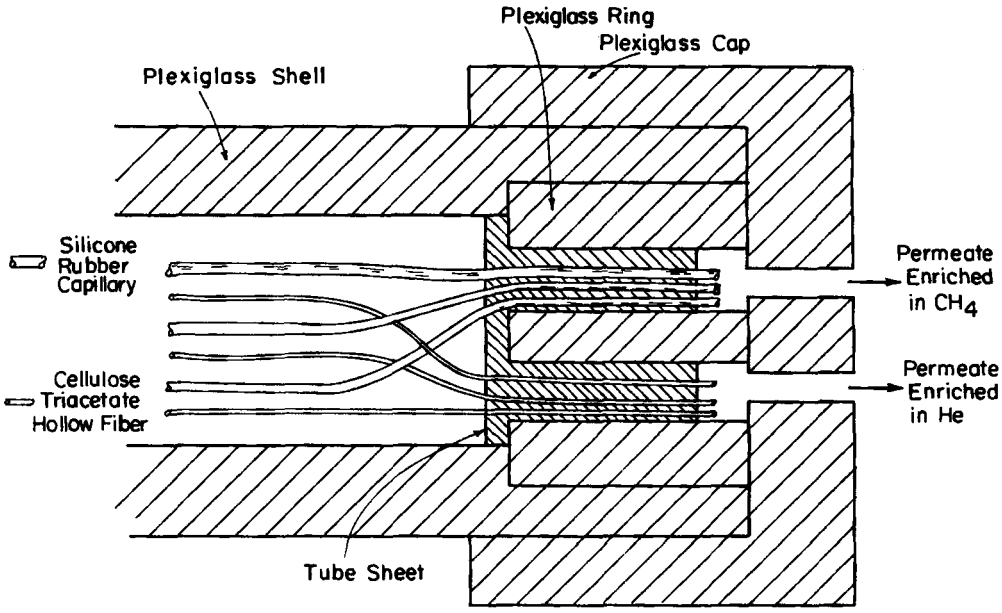

Figure 2. Cross section through end of two-membrane permeator.

supplier to be as follows:

Gas	Grade	Purity vol %
Helium	High purity	99.995 min.
Methane	Ultrahigh purity	99.97 min.
Nitrogen	Prepurified	99.998 min.

The gases were used without further purification.

Gas mixtures

Two different He—CH_4 mixtures were used. The gas mixtures were obtained from Air Products Co., Tamaqua, Pa. The following gas analyses were provided for each gas mixture by the supplier:

1.	Helium	1.01 mol %
	Methane	Balance
	Water vapor	<15 ppm
	Total hydrocarbons	<1 ppm
2.	Helium	9.95 mol %
	Methane	Balance
	Water vapor	<15 ppm
	Total hydrocarbons	<1 ppm

Membranes

Silicone Rubber. The silicone rubber [poly(dimethylsiloxane)] capillaries employed in this study were produced by Dow Corning Corp. of Midland, Mich., and marketed under the name Silastic Medical Grade Tubing. The silicone rubber was stated by the manufacturer to contain 32.25 ± 3 vol. % (51.66 wt. %) of a silica filler. The specific gravity of the polymer was 0.98 and that of the silica filler was 2.2.

The nominal diameters of the silicone rubber capillaries were 635 μm (2.5×10^{-2} in) OD and 305 μm (1.2×10^{-2} in) ID. These diameters were measured by microscopic observation. Additionally, the ID was found experimentally by determining the weight of mercury required to fill a selected length of capillary. The measured outer and inner diameters of the capillaries were found to be very close to their nominal values, which were used in all calculations.

Cellulose Triacetate. Asymmetric hollow fibers of cellulose triacetate were obtained in a water-wet state from Dow Chemical Co., Walnut Creek, Calif. The hollow fibers had to be dried prior to use in order to preserve their asymmetric character during the gas permeation studies. The method employed for this purpose was that described by MacDonald and Pan (1974).

The inner and outer diameters of the hollow fibers of cellulose triacetate were determined by electron microscopy because their bore was very small. Using eight samples, the OD of the hollow fibers was determined to be 245.0 ± 11 μm (9.65×10^{-3} in); the I.D. was found to be approximately 69.0 ± 3 μm (2.72×10^{-3} in). No specification for the nominal diameters was given by the manufacturer. However, the dimensions of the outer and inner diameters of these fibers have been reported by Pan et al. (1978) to be 225 μm (8.86×10^{-3} in) and 70 μm (2.76×10^{-3} in), respectively.

Experimental Results

Permeability coefficients for pure gases

Steady-state rates of permeation, $L_{o(\ell)}$, of He and CH_4 through symmetric dense capillaries of silicone rubber and through asymmetric hollow fibers of cellulose triacetate have been measured by means of the single-membrane permeators described in the previous section. The measurements were made at 30°C and at pressures $p_{(\ell)}$ in the range from 1.70×10^5 N/m^2 (25 psia) to about 3.77×10^5 N/m^2 (55 psia) at the high-pressure inlet of the permeators. The pressure $p_{(\ell)}$ at the low-pressure outlet was always close to atmospheric. It was estimated that the axial pressure drop in the permeator was not significant either shell-side or tube-side under the experimental conditions.

The experimental results are reported in terms of mean permeability coefficients $\bar{P}$, which are defined for tubular mem-

branes by the relation:

$$\bar{P} = \frac{L_{o(\ell)} \cdot \ln (r_o/r_1)}{2\pi \mathcal{L} \cdot \Delta p}, \tag{3}$$

where r_o and r_1 are the nominal outer and inner radii of the tubular membranes, $\mathcal{L}$ is the length of the tubular membranes, and $\Delta p [= p(\ell) - p_{(\ell)}]$ is the pressure drop across the walls of the membranes. When the walls of the tubular membranes are very thin, so that $r_o/r_1 \approx 1$, then:

$$\ln\left(\frac{r_o}{r_1}\right) \approx \frac{r_o - r_1}{r_o} \tag{4}$$

and Eq. 3 reduces to the form used for planar (sheet) membranes:

$$\bar{P} = L_{o(\ell)} \cdot \delta/A \cdot \Delta p, \tag{5}$$

where $\delta = (r_o - r_1)$ and A are the effective thickness and area of the membranes, respectively.

The results of the gas permeability measurements with silicone rubber capillaries ($r_o/r_1 = 2.083$) are presented in Figure 3 in the form of semilogarithmic plots of $\bar{P}$ for He and CH_4 as a function of Δp. The values of $\bar{P}$ were calculated from Eq. 3. The maximum error in $\bar{P}$ has been estimated to be $\pm 10\%$.

Similar results obtained with asymmetric hollow fibers of cellulose triacetate are presented in Figure 4. The effective thickness δ of these hollow fibers was that of their dense surface layer, or skin. Previous work with asymmetric hollow fibers of the same origin indicated that their skin was very thin (Pan et al., 1978), but the actual skin thickness of the hollow fibers employed in the present work was not known. Therefore, the results of the permeability measurements with the hollow fibers of cellulose triacetate are presented in Figure 4 in the form of semilogarithmic plots of $\bar{P}/\delta$ for He and CH_4 as a function of Δp. The values of $\bar{P}/\delta$ were calculated from Eq. 5 and their maximum error was estimated to be $\pm 8\%$.

An examination of Figure 3 shows that the permeability coefficients for He and CH_4 in silicone rubber capillaries are essentially independent of Δp under the conditions of this study. The value of $\bar{P}$ for He at 30°C agrees within 15% with that reported by Stern et al. (1965), and within 11% with that of Ohno et al. (1976). The value of $\bar{P}$ for CH_4 at the same temperature also agrees within 15% with that reported by Stern et al. (1965).

It is interesting to note that measurements of permeation rates of O_2, N_2, Ar, Kr, and Xe through silicone rubber capillaries of the same origin as those used in this study showed that $\bar{P}$ decreased with increasing Δp at 30°C. (Stern, et al., 1977; Stern and Leone, 1980). This behavior was attributed to the elastic deformation of the capillaries under external pressure, which resulted in an unequal decrease in their outer and inner diameters with an attendant increase in wall thickness. The present results did not reflect such a behavior, possibly because the scatter in the values of $\bar{P}$, which were obtained with three different permeator modules, was larger than the maximum expected decrease in $\bar{P}$ due to elastic deformation. Under the experimental conditions, this decrease was estimated to be about 5% at $\Delta p = 2.7 \times 10^5$ N/m^2 (40 psi), based on an average value of

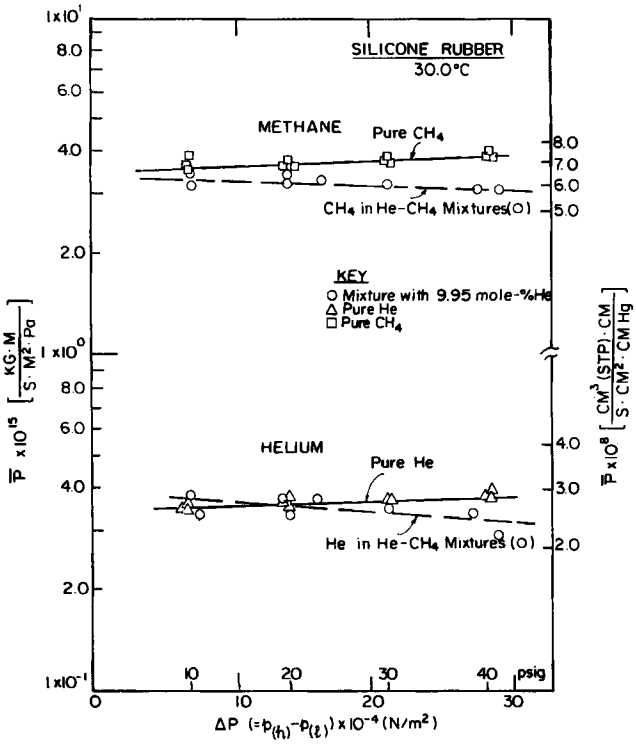

Figure 3. Permeability coefficients $\bar{P}$ for Helium and Methane in symmetric dense capillaries of silicone rubber at 30°C.

Straight lines are least-squares fits to experimental data.

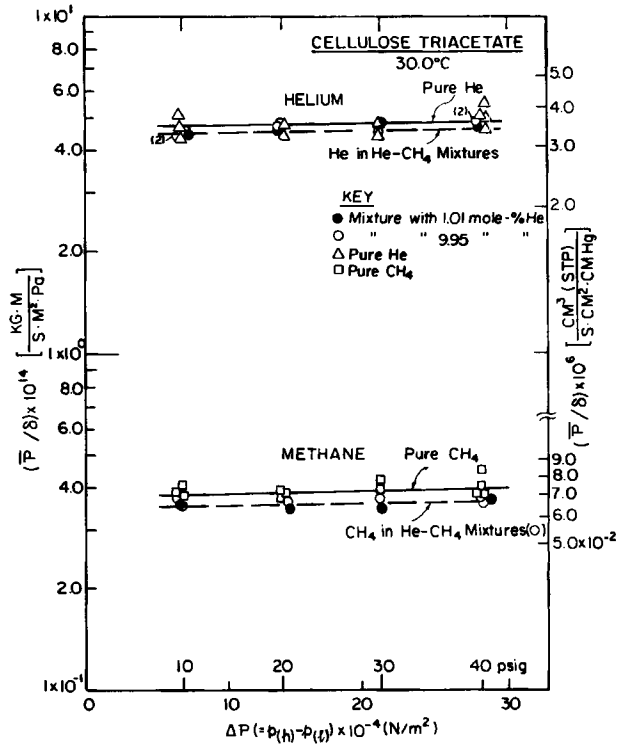

Figure 4. Permeability coefficients $\bar{P}/\delta$ for Helium and Methane in asymmetric hollow fibers of cellulose triacetate at 30°C.

Straight lines are least-squares fits to experimental data.

Young's modulus E of 3.09×10^6 N/m^2 (448 psi) for the silicone capillaries (Stern et al., 1977).

Figure 4 shows that the permeability coefficients for He and CH_4 in the asymmetric hollow fibers of cellulose triacetate are also independent of Δp under the conditions of this study. The values of $\bar{P}$ obtained for the two gases are an order of magnitude lower than those reported by MacDonald and Pan (1974) for hollow fibers of the same origin and under comparable conditions. However, the ideal separation factors $\alpha^*(He/CH_4) \equiv \bar{P}^{He}/\bar{P}^{CH_4}$ obtained in the two studies are more consistent: a mean value of $\alpha^* = 49$ was obtained in this study, while MacDonald and Pan obtained values of α^* in the range from about 40 to 60, depending on the solvents used in drying their hollow fibers.

The above observations suggest that the hollow fibers of cellulose triacetate used in the two studies differed mainly in the effective thickness of their dense skin. This difference probably was due, in turn, to some difference in the respective techniques employed in drying the hollow fibers. For example, MacDonald and Pan have shown that even very minor variations in the drying technique will significantly affect the values of gas permeability coefficients.

Permeability coefficients for gas mixtures

Steady-state rates of permeation of two different He—CH_4 mixtures through silicone rubber capillaries and through asymmetric hollow fibers of cellulose triacetate have been measured at 30°C and at the same pressures as used in the measurements with pure He and CH_4. The mixtures contained 1.01 and 9.95 mol % He, respectively, and the permeation rates were determined under the so-called perfect mixing conditions described previously.

Permeability coefficients for He and CH_4 were calculated from the permeation rates of the He—CH_4 mixtures and the compositions of the high- and low-pressure gas streams at the permeator outlets. Equations 3 and 5 were used for this purpose, except that $L_{o(\ell)}$ was replaced by $L^i_{o(\ell)}$, the flow rate of the individual components of the mixtures, i.e., $L^i_{o(\ell)} = y^i_o L_{o(\ell)}$, and Δp was replaced by Δp^i, the partial pressure difference of these components across the walls of the hollow fibers, i.e., $\Delta p^i = p_{(\ell)}x^i_o - p_{(\ell)}y^i_o$. The symbols x^i_o and y^i_o denote the mole fractions of component i (He or CH_4) in the unpermeated and permeated product streams, respectively, at the permeator outlets. Since the measurements were made under perfect mixing conditions, x^i_o and y^i_o are also the mole fractions of component i in the unpermeated and permeated streams, respectively, everywhere in a permeator module. Equation 3 was used for the measurements with silicone rubber capillaries, while Eq. 5 was used for the measurements with the hollow fibers of cellulose triacetate.

The permeability coefficients, $\bar{P}$ and $\bar{P}/\delta$, for He and CH_4 obtained from the measurements with the He—CH_4 mixtures are compared in Figures 3 and 4 with the permeability coefficients obtained with pure He and CH_4 at the same temperatures. The maximum error in the former values of $\bar{P}$ and P/δ has been estimated to be ±12%. Figures 3 and 4 show that the results of the permeability measurements with the mixtures agree within experimental error with those made with the pure gases. This behavior indicates that He and CH_4 do not interact in the permeating mixtures, as would be expected from the low solubility of the two gases in silicone rubber and in cellulose triacetate. The constancy of the permeability coefficients for He and CH_4 (within the experimental error) over the pressure range studied can also be attributed to the low solubility of these gases in the two polymers (Stern and Frisch, 1981).

Comparison of Experimental and Theoretical Results

Model description

The experimental results of this study on the separation of He—CH_4 mixtures in two-membrane permeators have been compared with the results predicted from the mathematical models of Perrin and Stern (1985), after these models were modified to take into account the use of asymmetric tubular membranes, such as asymmetric hollow fibers. The original models were based on the following assumptions:

1. Both types of membranes used in a two-membrane permeator are symmetric (dense).
2. The permeability coefficients for the components of a permeating mixture are the same as those of the pure components and, moreover, are independent of pressure.
3. The axial pressure drop in a permeator module is negligible both shell-side and tube-side.

The last two assumptions are satisfactory for the experimental conditions of this study (see below). The first assumption, however, had to be modified because the two-membrane permeators used in this study contained both symmetric and asymmetric membranes. The former were capillaries of silicone rubber while the latter were hollow fibers of cellulose triacetate. An asymmetric hollow fiber is visualized here as consisting of a highly porous, tubular substrate covered with a much thinner, dense surface layer or skin. The skin is an integral part of the hollow fiber. The separation of a gas mixture by selective permeation through asymmetric hollow fibers occurs almost entirely in the skin, which must be nonporous; the porous substrate provides the hollow fibers with the necessary mechanical strength. In the asymmetric hollow fibers employed in this study, the skin was formed on their external surfaces.

The mathematical models describing the separation of a binary gas mixture in a two-membrane permeator enclosing both symmetric and asymmetric membranes are presented in the Appendix for cocurrent and countercurrent operating conditions.

Separation of He—CH_4 mixtures

The separation of a He—CH_4 mixture containing 9.95 mol % He was studied in two-membrane permeators, which housed both symmetric dense capillaries of silicone rubber and asymmetric hollow fibers of cellulose triacetate, as detailed in Table 2. The He concentration in large natural gas streams in the United States is generally in the range from about 0.1 to 1.0 mol %. However, the use of gas mixtures with such a low He content in the present study would have resulted in a substantial experimental error.

The measurements were made at 30°C, at several applied pressures, and over a range of stage cuts θ_I and θ_{II}. The pressures were: $p_{(\ell)} = 1.70 \times 10^5$ N/m^2 (24.7 psia), 2.39×10^5 N/m^2 (34.7 psia), and 3.77×10^5 N/m^2 (54.7 psia); at the same time, the pressure $p_{(r)}$ was always near 1×10^5 N/m^2 (14.7 psia). The permeators were operated under perfect mixing, cocurrent flow, and countercurrent flow conditions. Different stage cuts were achieved by adjusting the feed flow rates. The accuracy of the measurements was ±3–5% (relative).

Typical experimental results are reported in Figures 5 to 9, where the compositions of the unpermeated (high-pressure) product stream and of the two permeated (low-pressure) product streams are shown as a function of the pressure difference $\Delta p\,[=p_{(\ell)} - p_{(\ell')}]$ and the stage cuts θ_I and θ_{II} for the three flow patterns in the permeators mentioned above. It should be noted that $\theta_I > \theta_{II}$ in Figure 5, $\theta_I \approx \theta_{II}$ in Figures 6 and 7, and $\theta_I < \theta_{II}$ in Figures 8 and 9.

The separation experiments were also simulated by means of the mathematical models presented in the Appendix for cocurrent and countercurrent operating conditions, and by a straightforward modification of the model for perfect mixing conditions derived for single-membrane permeators (Perrin and Stern, 1985). The permeability coefficients for He and CH_4 used in these calculations ($\overline{P}$ or $\overline{P}/\delta$) were those reported for the pure gases in Figures 3 and 4, since these agreed closely with the values obtained from permeability measurements with He—CH_4 mixtures. The axial pressure drop inside the silicone rubber capillaries was neglected, having been found to be insignificant for Δp values of less than 3.45×10^5 N/m^2 (50 psi) (Stern and Leone, 1980). The axial pressure drop inside the hollow fibers of cellulose triacetate was estimated to be less than 2% of the applied Δp under the experimental conditions (Pan and Habgood, 1978a), and was therefore also neglected.

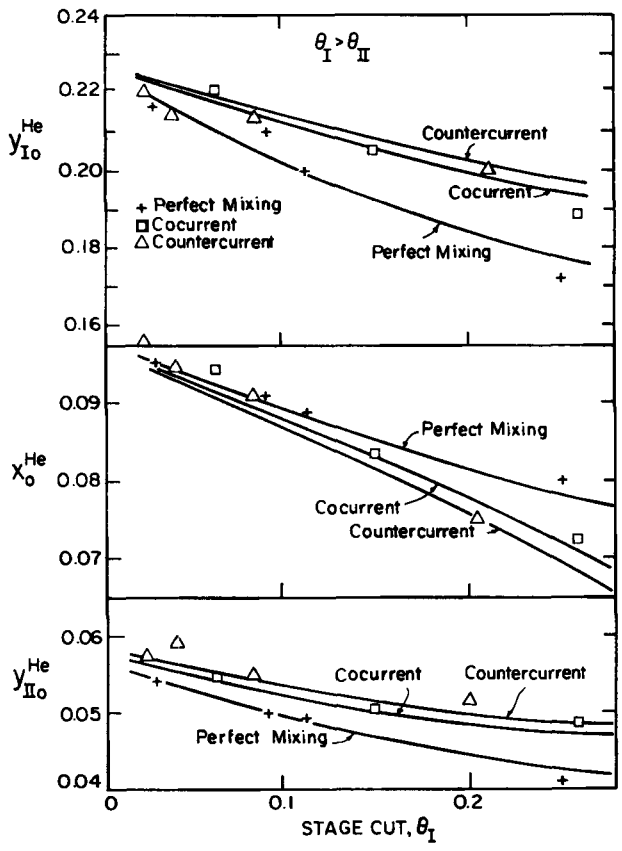

Figure 5. Separation of a He—CH_4 mixture in a two-membrane permeator at 30°C.

Membrane I: Asymmetric hollow fibers of cellulose triacetate.
Membrane II: Symmetric dense capillaries of silicone rubber.
Feed composition: 9.95 mol % He.
Operating conditions: $\theta_I \approx 2$ to $3\,\theta_{II}$, $\Delta p_I = \Delta p_{II} = 1.38 \times 10^5$ N/m^2 (20 psi).
Ratio of membrane areas: $A_I/A_{II} = 3.5$.
Curves show theoretical results.

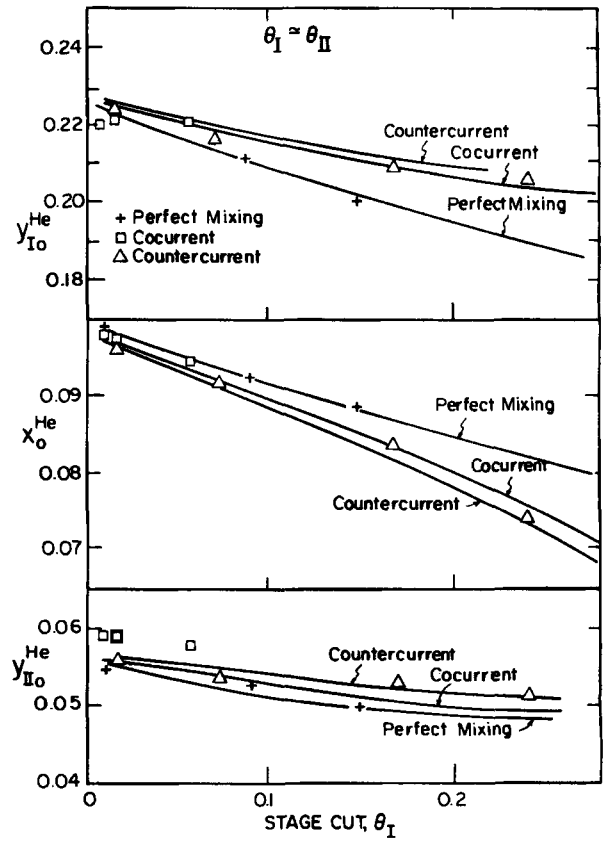

Figure 6. Separation of He—CH_4 mixture in a two-membrane permeator at 30°C.

Membranes and feed composition as in Fig. 5.
Operating conditions: $\theta_I \approx \theta_{II}$, $\Delta p_I = \Delta p_{II} = 1.38 \times 10^5$ N/m^2 (20 psi).
Ratio of membrane areas: $A_I/A_{II} = 3.5$.
Curves show theoretical results.

The theoretical and experimental results are compared in Figures 5 to 9; the theoretical results are represented by the curves in these figures. The two sets of data agree in general within ±20%, and in some cases within ±10%. This agreement probably is the best that can be expected, considering the simplifying assumptions made in the theoretical model and the magnitude of the experimental error. The agreement is better at the lower stage cuts, particularly when the value of the stage cut is smaller than that of the feed composition, x_f^{He}. It should be noted that under some experimental conditions the compositions of the three product streams, y_{Io}^{He}, y_{IIo}^{He}, and x_o^{He}, are only weakly dependent on the type of flow pattern used. However, the general trends are sufficiently clear to permit a meaningful comparison to be made between theory and experiment. The weak dependence of the product compositions on flow pattern is a consequence of the small stage cuts used in this study. Larger stage cuts would have resulted, however, in a lower extent of separation in some cases.

An examination of Figures 5 to 9 reveals the following permeation behavior:

1. When stage cut θ_I for membrane I becomes larger than stage cut θ_{II} for membrane II, the performance of a two-membrane permeator approaches that of a single-membrane permea-

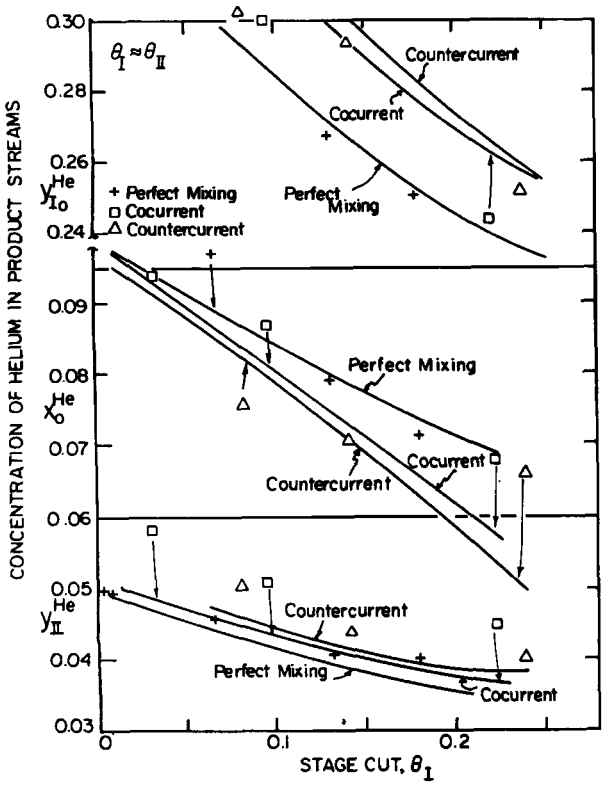

Figure 7. Separation of He—CH_4 mixture in a two-membrane permeator at 30°C.

Membranes and feed composition as in Fig. 5.
Operating conditions: $\theta_I \approx \theta_{II}$, $\Delta p_I = \Delta p_{II} = 2.76 \times 10^5$ N/m^2 (40 psi).
Ratio of membrane areas: $A_I/A_{II} = 3.5$.
Curves show theoretical results.

tor containing membrane I only. The most efficient flow pattern in a single-membrane permeator, i.e., the pattern that yields the highest separation and requires the smallest membrane area, is countercurrent flow, followed by cross-flow, cocurrent flow, and perfect mixing (Walawender and Stern, 1972). A two-membrane permeator operating under conditions where $\theta_I > \theta_{II}$ should exhibit a similar behavior. Figure 5 shows that countercurrent and cocurrent flow yield indeed a higher separation than perfect mixing in a two-membrane permeator operating with $\theta_I > \theta_{II}$; in Figure 5, θ_I is approximately two to three times larger than θ_{II}. The extent of separation achieved is best characterized by the value of y^{He}_{Io}, the He mole fraction concentration in the permeate from membrane I (the asymmetric hollow fibers of cellulose triacetate). In the present study the terms countercurrent and cocurrent apply strictly only to the flow patterns at the interfaces of the two membranes in the permeator. The separation of the feed mixture actually occurred under flow conditions that are better described as cross-flow/countercurrent and cross-flow/cocurrent, the cross-flow taking place in the asymmetric membrane I.

2. The above trends, which were found for conditions when $\theta_I > \theta_{II}$, were also observed when $\theta_I \approx \theta_{II}$. However, the He concentration in the permeate from membrane I, y_{Io}, was higher for $\theta_I \approx \theta_{II}$, as can be seen by comparing Figures 5 and 6 for $\Delta p = 1.38 \times 10^5$ N/m^2 (20 psi) (in this study, $\Delta p = \Delta p_I = \Delta p_{II}$).

Whatever the relative values of θ_I and θ_{II}, the separation is generally enhanced by an increase in the pressure drop Δp across either of the two membranes, or across both membranes. This is seen from Figure 6 [$\Delta p = 1.38 \times 10^5$ N/m^2 (20 psi)] and Figure 7 [$\Delta p = 27.6 \times 10^5$ N/m^2 (40 psi)]. The He concentration in the permeate from membrane I, y^{He}_{Io}, is significantly higher for $\Delta p = 40$ psi than for $\Delta p = 20$ psi, when compared at the same stage cuts.

3. One of the most striking conclusions derived from the theoretical models (Perrin and Stern, 1985) was that in cases where $\theta_I \ll \theta_{II}$, perfect mixing would yield a better separation than other flow patterns. This is never the case in single-membrane permeators. The above prediction appears to be confirmed by the results presented in Figure 8 and, particularly, in Figure 9, where $\theta_I \approx 0.1\ \theta_{II}$. Although the experimental results obtained with the three flow patterns studied are close to each other, the He concentration in the permeate from membrane I, y^{He}_{Io}, for perfect mixing is seen to be equal to or higher than that for countercurrent or cocurrent flow. Moreover, when $\theta_I \ll \theta_{II}$, the He concentration in the permeated product stream from membrane I increases with increasing θ_I, as predicted by the theoretical model. In contrast, when $\theta_I > \theta_{II}$ or $\theta_I \approx \theta_{II}$ the He concentration in this stream decreases with increasing θ_I; see Figures 5–7. Figures 8 and 9 also show that for $\theta_I \ll \theta_{II}$, the concentration of He in the unpermeated (high-pressure) product stream increases with increasing stage cut θ_I. This behavior never occurs in a single-membrane permeator.

An interesting application of two-membrane permeators such

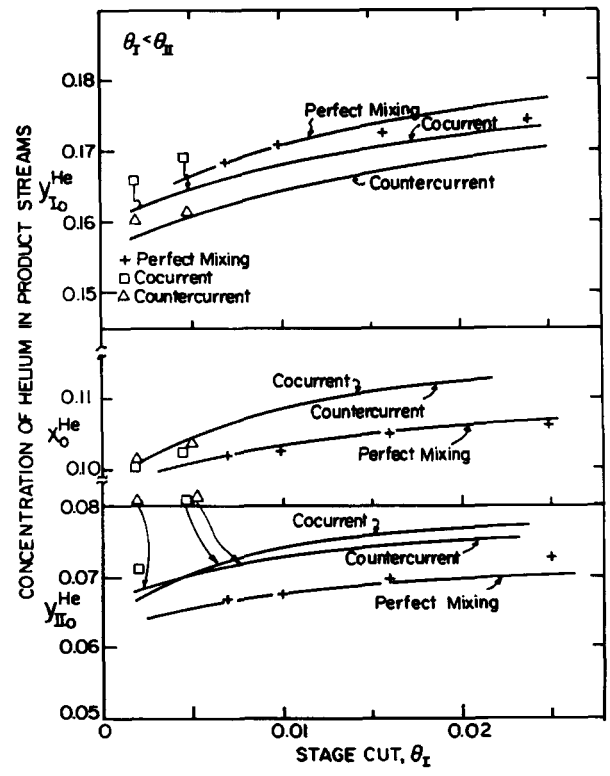

Figure 8. Separation of He—CH_4 mixture in a two-membrane permeator at 30°C.

Membranes and feed composition as in Fig. 5.
Operating conditions: $\theta_I \approx 0.1\ \theta_{II}$, $\Delta p_I = \Delta p_{II} = 0.69 \times 10^5$ N/m^2 (10 psi).
Ratio of membrane areas: $A_I/A_{II} = 1.9$.
Curves show theoretical results.

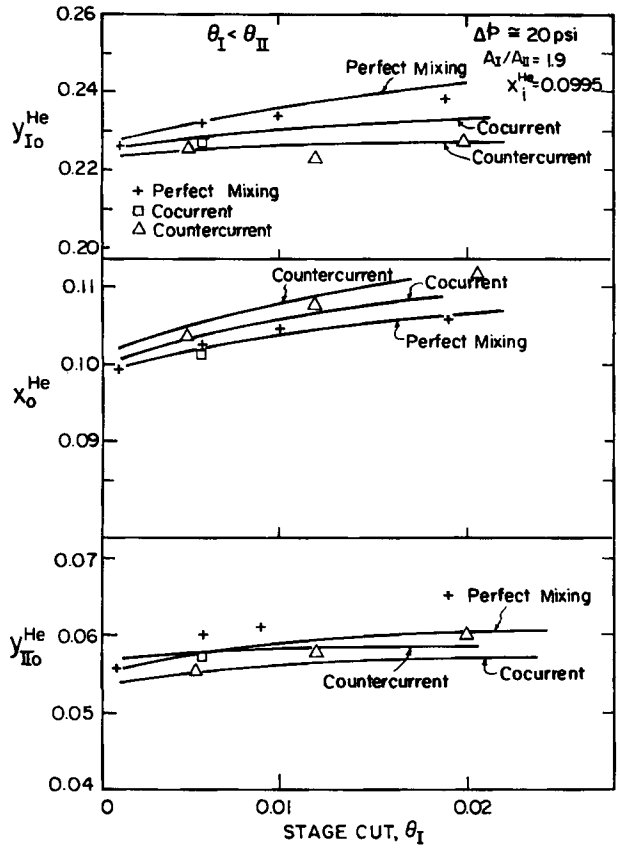

Figure 9. Separation of a He—CH_4 mixture in a two-membrane permeator at 30°C.

Membranes and feed composition as in Fig. 5.
Operating conditions: $\theta_I \approx 0.1\ \theta_{II}$, $\Delta p_I = \Delta p_{II} = 1.38 \times 10^5$ N/m^2 (20 psi).
Ratio of membrane areas: $A_I/A_{II} = 1.9$.
Curves show theoretical results.

as those described above would be for the recovery of He from natural gas. The theoretical models indicate that the concentration of He in the permeate stream from, say, membrane I (which must be He-selective) could be greatly enhanced by the presence of a second membrane with a reverse gas selectivity, provided that:

1. The selectivity of membrane II toward CH_4, relative to He, is sufficiently large.
2. The stage cut θ_{II} for membrane II is also sufficiently large.

These conditions were only partially satisfied in the present study, in which the main objective was to test the validity of the theoretical models of two-membrane permeators. Thus, the selectivity of the silicone rubber capillaries (membrane II) toward CH_4 relative to He was not sufficiently high (see Figure 3) to significantly increase the He concentration in the permeated stream produced by the hollow fibers of cellulose triacetate (membrane I). Moreover, the measurements were made at relatively low values of θ_{II}.

The potential usefulness of two-membrane permeators is illustrated in Table 3 for the separation of a He—CH_4 mixture containing 9.95 mol % He. The selected operating conditions are stated in Table 3. The pertinent mathematical model predicts that for the membranes used in the present study, the He concentration in the permeated product stream from membrane I should increase with increasing θ_{II} from 24.24 mol % at θ_{II} = 0.201 to 33.33 mol % at θ_{II} = 0.80, θ_I being maintained constant at 0.019. The ideal separation factors used in this calculation were extracted from Figures 3 and 4. For θ_I = 0.019 and θ_{II} = 0.201, the model predicts that the above-mentioned product stream should contain 24.24 mol % He, which is in satisfactory agreement with the value of 23.8 mol % He obtained experimentally for the same conditions.

If the silicone rubber capillaries (membrane II), for which α_{II}^* (He/CH_4) = 0.376 at 30°C, Figure 3, could be replaced with a more highly CH_4-selective membrane with α_{II}^* = 0.0213, the He concentration in the permeated product stream from membrane I would vary from 27.16 mol % at θ_{II} = 0.201 to as much as 73.96 mol % at θ_{II} = 0.80, with θ_I still constant at 0.019. In contrast, a single-membrane permeator provided just with hollow fibers of cellulose triacetate (membrane I) could produce a permeate containing only 21.6 mol % He at θ_I = 0.019 (θ_{II} = 0), the other conditions being those specified in Table 3.

Consequently, the separation of a binary gas mixture by selective permeation could be greatly enhanced by the simultaneous use of two different membranes with sufficiently high reversed gas selectivities, if such membranes can be developed.

Conclusions

The separation of a He—CH_4 mixture achieved in two-membrane permeators was found to be consistent with the performance predicted by the mathematical models, particularly at the lower stage cuts. The experimental results confirmed the prediction that the highest separation is obtained when the two-membrane permeators are operated under either countercurrent or so-called perfect mixing flow conditions, depending on the relative values of the two stage cuts.

The models show that much higher separations can be achieved in two-membrane permeators than in permeators provided with a single type of membrane (Perrin and Stern, 1985).

Table 3. Effect of Ideal Separation Factors on Separation of a He-CH_4 Mixture in a Two-Membrane Permeator

Stage Cut for Membrane II† θ_{II}	Predicted Compositions of Product Streams, mol % He: Permeated Stream from Membrane I	Permeated Stream from Membrane II	Unpermeated Stream
(1) α_I^* (He/CH_4) = 47, α_{II}^* (He/CH_4) = 0.376			
0.201	24.24‡	5.85	10.66
0.40	26.73	6.51	11.77
0.50	28.17	6.70	12.41
0.60	29.73	7.32	13.11
0.80	33.33	8.31	14.73
(2) α_I^* (He/CH_4) = 47; $\alpha_{II}^* = (\alpha_I^*)^{-1}$ = 0.0213 (hypothetical value)			
0.201	27.16	0.54	11.96
0.50	40.77	0.94	18.10
0.60	48.67	1.23	21.76
0.80	73.96	2.85	34.61

Membrane I: Cellulose triacetate, asymmetric hollow fibers
Membrane II: Silicone rubber, symmetric (dense) capillaries
†Stage cut for membrane I: θ_I = 0.019
Feed composition: 9.95 mol % He
Pressure drop across membranes: 1.38 × 10^5 N/m^2 (20 psi)
Temperature: 30°C
Perfect mixing flow conditions
‡Experimental value: 23.8 mol % He

However, the separation efficiency of two-membrane permeators becomes significant only when the reverse selectivities of the two types of membrane toward the components of a binary gas mixture are sufficiently large and the stage cuts are properly adjusted.

The described membrane separation technique could be applied in principle also to the separation of multicomponent mixtures if membranes that exhibit specific selectivities toward the different components of the mixtures can be found.

Instead of using a single permeator module enclosing two or more different types of membranes it is also possible to employ two or more permeators, connected in various configurations, each containing a single (but different) type of membrane. A study of these alternatives has shown that the single permeator with multiple types of membranes is the most efficient configuration from the viewpoint of achievable separation under comparable operating conditions (Stern, et al., 1984).

Acknowledgment

The financial support of Dow Corning Corp. is gratefully acknowledged. The authors are also grateful to F. W. Gordon Fearon for useful discussions.

Notation

A = membrane area
a, b, c = constants, Eq. A4
$C_{\mathrm{I}}^{A,B}$ = expression defined by Eq. A1 or A2
$C_{\mathrm{II}}^{A,B}$ = expression defined by Eq. A5 or A6
$\mathcal{L}$ = length of capillaries or hollow fibers
L = local molar flow rate of unpermeated (high-pressure) stream
$L_{\mathrm{I,II}}$ = local molar flow rate on low-pressure side of membrane I or II
$L_{i(\ell)}$ = molar flow rate of unpermeated (high-pressure) stream at permeator (stage) inlet
$L_{o(\ell)}$ = molar flow rate of unpermeated (high-pressure) stream at permeator (stage) outlet
$L_{\mathrm{I,II}_{o(\ell)}}$ = molar flow rate of permeated (low-pressure) streams at permeator (stage) outlet
N = number of hollow fibers in permeator
$\bar{P}$ = mean permeability coefficient
$p_{(\ell)}$ = total pressure (absolute) on high-pressure side of membranes I and II
$p_{\mathrm{I}(\ell)}$ = total pressure (absolute) on low-pressure side of membrane I
$p_{\mathrm{II}(\ell)}$ = total pressure (absolute) on low-pressure side of membrane II
$r_{\mathrm{I,II}}$ = pressure ratio, $p_{(\ell)}/p_{\mathrm{I}(\ell)}$ or $p_{(\ell)}/p_{\mathrm{II}(\ell)}$
R = ratio of membrane areas, $A_{\mathrm{II}}/A_{\mathrm{I}}$
$x^{A,B}$ = local mole fraction of component A or B in unpermeated (high-pressure) stream
$x_i^{A,B}$ = mole fraction of component A or B in feed stream at permeator inlet
$y^{A,B}$ = local mole fraction of component A or B in permeated (low-pressure) stream
y' = local concentration of more rapidly permeating component (A) due only to component flux through membrane

Greek letters

α^* = ideal separation factor, $\bar{P}^A/\bar{P}^B$
δ = effective membrane thickness
θ_{I} = stage cut from membrane I, $L_{\mathrm{I}_{o(\ell)}}/L_{i(\ell)}$
θ_{II} = stage cut for membrane II, $L_{\mathrm{II}_{o(\ell)}}/L_{i(\ell)}$

Subscripts

ℓ = high-pressure side of membrane
i = permeator (stage) inlet
I = membrane (of type) I or low-pressure side of membrane I
II = membrane (of type) II or low-pressure side of membrane II
ℓ = low-pressure side of membrane
o = permeator (stage) outlet

Superscripts

A,B = component of gas mixture
i = component of gas mixture

Appendix

Perrin and Stern (1985) have developed mathematical models to describe the separation of binary gas mixtures in two-membrane permeators operating under perfect mixing, cocurrent flow, and countercurrent flow conditions. These models were derived for a permeator in which both types of membrane are symmetric (dense) in nature. However, the two-membrane permeators used in this study enclosed both symmetric and asymmetric membranes. As was shown by Pan (1983), the separation of gas mixtures by means of an asymmetric membrane must be described by a cross-flow model (Stern and Walawender, 1969), irrespective of whether the high- and low-pressure gas streams at the interfaces of the membrane flow cocurrently or countercurrently to one another. The cross-flow pattern is due to the fact that a gas permeating through the skin at one interface of an asymmetric membrane must traverse its porous substrate, in a direction roughly perpendicular to the skin, before reaching the opposite interface. Therefore, the models of Perrin and Stern were modified accordingly and the results are presented below. In the analysis that follows, membrane I will be considered as being asymmetric, while membrane II will be regarded as symmetric.

Cocurrent flow combined with cross-flow

The differential form of Fick's law, which describes the transport of components A and B through membrane I under cross-flow conditions, is:

$$y'dL_{\mathrm{I}} = (\bar{P}_{\mathrm{I}}^A/\delta_{\mathrm{I}})[p_{(\ell)}x^A - p_{\mathrm{I}(\ell)}y']dA_{\mathrm{I}} = C_{\mathrm{I}}^A dA_{\mathrm{I}} \quad \text{(A1)}$$

$$(1 - y')dL_{\mathrm{I}} = (\bar{P}_{\mathrm{I}}^B\delta_{\mathrm{I}}) \cdot [p_{(\ell)}(1 - x^a) - p_{\mathrm{I}(\ell)}(1 - y')]dA = C_{\mathrm{I}}^B dA_{\mathrm{I}} \quad \text{(A2)}$$

As is shown in Figure 10, y' represents the local concentration of component A in the gas permeating through the differential membrane area dA_{I} (different from the local bulk permeate concentration y_{I}^A), and x^A is the local concentration of the unpermeated stream. L_{I} and L are the flow rates of the permeated and unpermeated streams, respectively. The symbols $\bar{P}$, δ, $p_{(\ell)}$, and $p_{\mathrm{I}(\ell)}$ have been defined previously. The ratio of Eq. A1 to Eq. A2 yields:

$$y'/(1 - y') = \alpha_{\mathrm{I}}^*(r_{\mathrm{I}}x^A - y')/[r_{\mathrm{I}}(1 - x^A) - (1 - y')], \quad \text{(A3)}$$

where $\alpha_{\mathrm{I}}^*(=\bar{P}_{\mathrm{I}}^A/\bar{P}_{\mathrm{I}}^B)$ is the ideal separation factor, and $r_{\mathrm{I}}(=p_{(\ell)}/p_{\mathrm{I}(\ell)}$ is the pressure ratio across membrane I.

The solution of Eq. A3 to yield y' as a function of the local unpermeated stream concentration x^A is (Stern and Walawender, 1969):

$$y' = f(x^A) = [b - (b^2 - 4ac)^{1/2}]/2a, \quad \text{(A4)}$$

where

$$a = \alpha_{\mathrm{I}}^* - 1,$$

$$b = r_{\mathrm{I}} + \alpha_{\mathrm{I}}^*(r_{\mathrm{I}}x^A + 1),$$

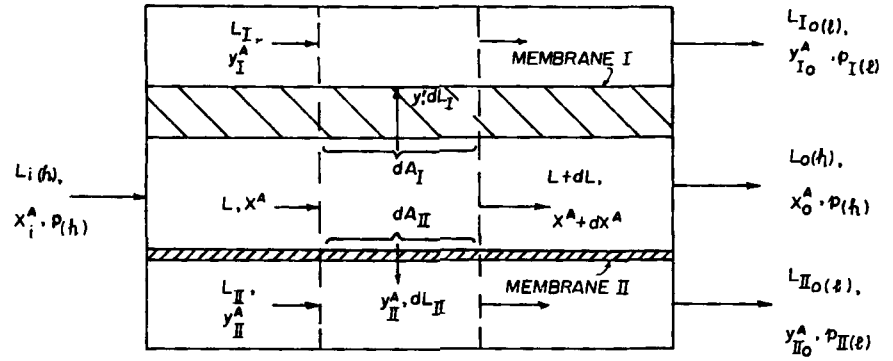

Figure 10. Diagram of two-membrane permeator with cocurrent gas flow.

Flow at membrane interfaces is cocurrent; separation of gas mixture in asymmetric membrane I is by cross-flow. Thickness of membrane I exaggerated compared to membrane II for clarity. Membrane II is symmetric (dense).

and

$$c = \alpha_I^* r_I x^A$$

For membrane II, which is symmetric (dense), the transport equations for cocurrent flow conditions are (Perrin and Stern, 1985):

$$d(y_{II}^A L_{II}) = (\bar{P}_{II}^A/\delta_{II})[p_{(\ell)}x^A - p_{II(\ell)}y_{II}^A]dA_{II} = C_{II}^A dA_{II} \quad \text{(A5)}$$

$$d[(1 - y_{II}^A)L_{II}] = (\bar{P}_{II}^B/\delta_{II})[p_{(\ell)}(1 - x^A] - p_{II(\ell)}(1 - y_{II}^A)]dA_{II} = C_{II}^B dA_{II}, \quad \text{(A6)}$$

where L_{II} and y_{II}^A are the local molar flow rate of the permeated stream and the concentration of component A in that stream associated with membrane II, respectively. The relation between dA_I and dA_{II} is $dA_{II} = RdA_I$, where R is a constant that can be related to the geometry of the membranes (Perrin and Stern, 1985).

In addition to these equations, several material balances can be written around the permeator from the inlet to a position z; see Figure 11. These balances include:

$$L_{i(\ell)} = L_I + L_{II} + L, \quad \text{(A7a)}$$

$$L_{i(\ell)}x_i^A = L_I y_I^A + L_{II} Y_{II}^A + Lx^A, \quad \text{(A7b)}$$

and

$$0 = dL_I + dL_{II} + L \quad \text{(A7c)}$$

Moreover,

$$x^A L = (L + dL)(x^A + dx^A) + y'dL_I + d(L_{II}y_{II}^A), \quad \text{(A8a)}$$

and

$$(y_I^A + dy_I^A)(L_I + dL_I) = y_I^A L_I + y'dL_I \quad \text{(A8b)}$$

Neglecting second-order terms, a rearrangement of Eqs. A8a and A8b yields:

$$dx^A/dL_I = -[x^A dL/dL_I + y' + d(L_{II}y_{II}^A)/dL_I]/L \quad \text{(A9a)}$$

$$dy_I^A/dL_I = (y' - y_I^A)/L_I \quad \text{(A9b)}$$

If L_I is the independent variable, Eqs. A1 through A9 contain all the information necessary to derive the equations for y_I^A, y_{II}^A,

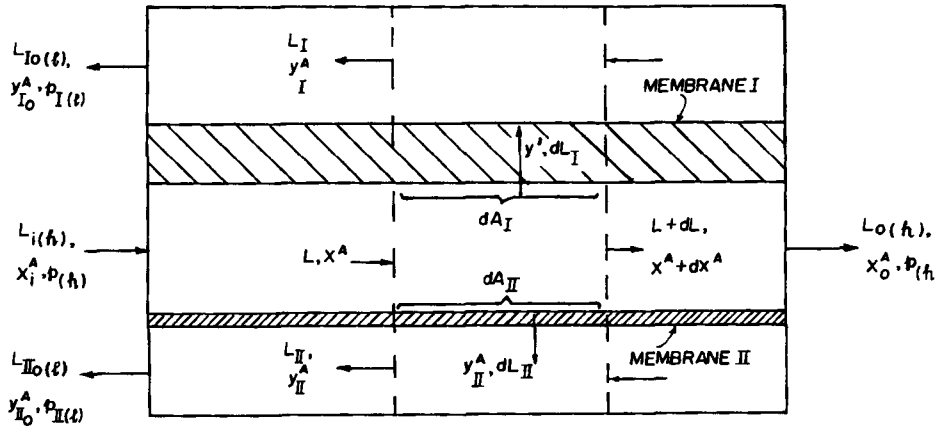

Figure 11. Diagram of two-membrane permeator with countercurrent gas flow.

Flow at membrane interfaces is countercurrent; separation of gas mixture in asymmetric membrane I is by cross-flow. Thickness of membrane I exaggerated compared to membrane II for clarity. Membrane II is symmetric (dense).

L, L_{II}, x^A, A_I, and A_{II}:

$$dA_I/dL_I = y'/C_I^A \quad \text{(A10)}$$

$$dA_{II}/dL_I = RdA_I/dL_I \quad \text{(A11)}$$

$$dy_I/dL_I = (y' - y_I^A)/L_I \quad \text{(A12)}$$

$$dL_{II}/dL_I = Ry'(C_{II}^A + C_{II}^B)/C_I^A \quad \text{(A13)}$$

$$dL/dL_I = -(1 - dL_{II}/dL_I) \quad \text{(A14)}$$

$$dx^A/dL_I = -(x^A dL/dL_I + y' + y'RC_{II}^A/C_I^A)/L \quad \text{(A15)}$$

$$y' = f(x^A) \quad \text{(A16)}$$

$$L = L_{i(\ell)} - L_I - L_{II} \quad \text{(A17)}$$

$$y_{II}^A = (L_{i(\ell)}x_i^A - Lx^A - L_I y_I^A)/L_{II} \quad \text{(A18)}$$

The above equations are integrated from the permeator inlet, where the boundary conditions are:

$$L = L_{i(\ell)} \quad \text{(A19)}$$

$$A_I = A_{II} = 0 \quad \text{(A20)}$$

$$L_I = L_{II} = 0 \quad \text{(A21)}$$

$$y_I^A = y' \quad \text{(A22)}$$

$$x^A = x_i^A, \quad \text{(A23)}$$

where y' is determined from Eq. A4 for $x^A = x_i^A$, and y_{II}^A is obtained from a similar expression (Eq. 24b, Perrin and Stern, 1985).

Because dy_I^A/dL_I is indeterminate at the permeator inlet, L'Hospital's rule is used to give:

$$dy_I^A/dL_I = \tfrac{1}{2}dy'/dL_I = \tfrac{1}{2}(dy'/dx^A) \cdot (dx^A/dL_I), \quad \text{(A24)}$$

where dy'/dx^A is determined from the differentiation of Eq. A4.

Countercurrent flow combined with cross-flow

The following equations apply to countercurrent flow in a two-membrane permeator with asymmetric and symmetric membranes. From Figure 11, the mass balances around the permeator from the permeator outlet to some position z are:

$$L = L_{o(\ell)} + L_I + L_{II} \quad \text{(A25)}$$

$$Lx^A = L_{o(\ell)}x_o^A + L_I y_I^A + L_{II}y_{II}^A \quad \text{(A26)}$$

$$dL = dL_I + dL_{II} \quad \text{(A27)}$$

$$d(Lx^A) = d(L_I y_I^A) + d(L_{II}y_{II}^A) \quad \text{(A28)}$$

which gives for the governing equations:

$$dA_I/dL_I = y'/C_I^A \quad \text{(A29)}$$

$$dA_{II}/dL_I = RdA_I/dL_I \quad \text{(A30)}$$

$$dy_I/dL_I = (y' - y_I^A)/L_I \quad \text{(A31)}$$

$$dL_{II}/dL_I = Ry'(C_{II}^A + C_{II}^B)/C_I^A \quad \text{(A32)}$$

$$dL/dL_I = (1 + dL_{II}/dL_I) \quad \text{(A33)}$$

$$dx^A/dL_I = (-x^A dL/dL_I + y' + y'RC_{II}^A/C_I^A)/L \quad \text{(A34)}$$

$$y' = f(x^A) \quad \text{(A35)}$$

$$L = L_{o(\ell)} + L_I + L_{II} \quad \text{(A36)}$$

$$y_{II}^A = (Lx^A - L_{o(\ell)}x_o^A - L_I y_I^A)/L_{II} \quad \text{(A37)}$$

These equations are integrated from the permeator outlet, where the boundary conditions are:

$$x^A = x_o^A \quad \text{(A38)}$$

$$L = L_{o(\ell)} \quad \text{(A39)}$$

The integration procedures to solve the differential equations for cocurrent and countercurrent flow have been described elsewhere (Perrin and Stern, 1985).

Literature cited

Blaisdell, C. T., and K. Kammermeyer, "Countercurrent and Cocurrent Gas Separation," *Chem. Eng. Sci.*, **28**, 1249 (1973).

Breuer, M. E., and K. Kammermeyer, "Effect of Concentration Gradient in Barrier Separation Cells," *Separ. Sci.*, **2**, 319 (1967).

Hill, C. G., *An Introduction to Chemical Engineering Kinetics and Reactor Design*, Wiley, New York, 397 (1977).

Hwang, S.-T., and K. Kammermeyer, *Membranes in Separations*, Wiley-Interscience, New York (1975).

Kimura, S., T. Nomura, T. Miyauchi, and M. Ohno, "Separation of Rare Gases by Membranes," *Radiochem. Radioanal. Lett.*, **13**, 349 (1973).

McAfee, K. B., *Encyclopedia of Chemical Technology*, A. Stauden, ed., Supp. 2, pp. 297–315, Interscience, New York (1960).

MacDonald, W. R., and C.-Y. Pan, U.S. Pat. 3,842,515 (1974).

Ohno, M., T. Morisue, O. Ozaki, H. Heki, and T. Miyauchi, "Separation of Rare Gases by Membranes," *Radiochem. Radioanal. Lett.*, **27**, 299 (1976).

Ohno, M., O. Ozaki, and H. Sato, "Radioactive Rare Gas Separation Using a Separation Cell with Two Kinds of Membranes Differing in Gas Permeability Tendency," *J. Nucl. Sci. Technol. Japan*, **14**, 589 (1977).

Ohno, M., T. Morisue, O. Ozaki, and T. Miyauchi, "Radioactive Rare Gas Separation, Performance of a Two-Unit Series-Type Separation Cell," *J. Nucl. Sci. Technol. Japan*, **15**, 411 (1978a).

Ohno, M., H. Heki, O. Ozaki, and T. Miyauchi, "Radioactive Rare Gas Separation, Performance of a Two-Unit Series-Type Separation Cell, *J. Nucl. Sci. Technol. Japan*, **15**, 668 (1978b).

Oishi, J., Y. Matsumura, K. Higashi, and C. Ike, "Analysis of a Gaseous Diffusion Separation Unit," *J. Atomic Energy Soc. (Japan)*, **3**, 923 (1961); U.S. Atomic Energy Commission Report AEC-TR-5134.

Pan, C.-Y., "Gas Separation by Permeators with High-Flux Asymmetric Membranes," *AIChE J.*, **29**, 545 (1983).

Pan, C.-Y., C. D. Jensen, C. Bielech, and H. W. Habgood, "Permeation of Water Vapor through Cellulose Triacetate Membranes in Hollow Fiber Form," *J. Appl. Polym. Sci.*, **22**, 2307 (1978).

Pan, C.-Y., and H. W. Habgood, "An Analysis of the Single-Stage Gaseous Permeation Process," *Ind. Eng. Chem. Fundam.*, **13**, 323 (1974).

———, "Gas Separation by Permeation. I: Calculation Methods and Parametric Analysis," *Can. J. Chem. Eng.*, **56**, 197 (1978a).

———, "Gas Separation by Permeation. II: Effect of Permeate Pressure Drop and Choice of Permeate Pressure," *Can. J. Chem. Eng.*, **56**, 210 (1978b).
Perrin, J. E., "Separation of Gas Mixtures in Permeators with Two Different Types of Membranes," Ph.D. Diss., Dept. Chem. Eng. and Mat. Sci., Syracuse Univ., Syracuse, NY (1986).
Perrin, J. E., and S. A. Stern, "Modeling of Permeators with Two Different Types of Membranes," *AIChE J.*, **31**, 1167 (1985).
Sengupta, A., and K. K. Sirkar, "Multicomponent Gas Separation by an Asymmetric Permeator Containing Two Different Membranes," *J. Membrane Sci.*, **21**, 73 (1984).
Sirkar, K. K., "Asymmetric Permeators—A Conceptual Study," *Separ. Sci. Techn.*, **15**, 1091 (1980).
Stern, S. A., and H. L. Frisch, "The Selective Permeation of Gases through Polymers," *Ann. Rev. Mater. Sci.*, **11**, 523 (1981).
Stern, S. A., and S. M. Leone, "Separation of Krypton and Xenon by Selective Permeation," *AIChE J.*, **26**, 881 (1980).
Stern, S. A., and W. P. Walawender, "Analysis of Membrane Separation Parameters," *Separ. Sci.*, **4**, 129 (1969).
Stern, S. A., and S.-C. Wang, "Countercurrent and Cocurrent Gas Separation in a Permeator Stage. Comparison of Computation Methods," *J. Membrane Sci.*, **4**, 141 (1978).
Stern, S. A., F. J. Onorato, and C. Libove, "The Permeation of Gases through Hollow Silicone Rubber Fibers: Effect of Fiber Elasticity on Gas Permeability," *AIChE J.*, **23**, 567 (1977).
Stern, S. A., J. E. Perrin, and E. J. Naimon, "Recycle and Multimembrane Permeators for Gas Separation," *J. Membrane Sci.*, **20**, 25 (1984).
Stern, S. A., T. F. Sinclair, P. J. Gareis, N. P. Vahldieck, and P. H. Mohr, "Helium Recovery by Permeation," *Ind. Eng. Chem.*, **57**, 49 (1965).
Walawender, W. P., and S. A. Stern, "Analysis of Membrane Separation Parameters. II: Countercurrent and Cocurrent Flow in a Single Permeation Stage," *Separ. Sci.*, **7**, 553 (1972).
Weller, S., and W. A. Steiner, "Separation of Gases by Fractional Permeation through Membranes," *J. Appl. Phys.*, **21**, 279 (1950a).
———, "Fractional Permeation through Membranes," *Chem. Eng. Prog.*, **46**, 585 (1950b).

Manuscript received Aug. 15, 1985, and revision received Mar. 20, 1986.